

Showcasing research from the Max Planck Institute for Chemical Energy Conversion and the group of Professor Jennifer Strunk, Leibniz Institute for Catalysis, Germany

The fate of  $O_2$  in photocatalytic  $CO_2$  reduction on  $TiO_2$  under conditions of highest purity

This study is dedicated to understanding the often-reported absence of gaseous  $O_2$  during photocatalytic conversion of  $CO_2$  and  $H_2O$  to  $CH_4$  over  $TiO_2$ -photocatalysts. While  $IrO_x$ -modified P25- $TiO_2$  allowed the detection of  $O_2$  and  $H_2$  in almost stoichiometric amounts, the results simultaneously imply that hydrogen for the  $CH_4$  formation does not result from complete water oxidation. A lack of gaseous  $O_2$  over unmodified P25- $TiO_2$  stems from a consumption of O-derived species by  $TiO_2$ .

As featured in:



See Simon Ristig,  
Jennifer Strunk *et al.*,  
*Phys. Chem. Chem. Phys.*,  
2019, 21, 15949.



Cite this: *Phys. Chem. Chem. Phys.*,  
2019, 21, 15949

# The fate of O<sub>2</sub> in photocatalytic CO<sub>2</sub> reduction on TiO<sub>2</sub> under conditions of highest purity†

Martin Dilla,<sup>a</sup> Alina Jakubowski,<sup>a</sup> Simon Ristig,<sup>id</sup>\*<sup>a</sup> Jennifer Strunk<sup>id</sup>\*<sup>b</sup> and Robert Schlögl<sup>ac</sup>

Although the photocatalytic reduction of CO<sub>2</sub> to CH<sub>4</sub> by using H<sub>2</sub>O as the oxidant presupposes the formation of O<sub>2</sub>, it is often not included in the product analysis of most of the studies dealing with photocatalytic CO<sub>2</sub> reduction or it is reported to be not formed at all. The present study aims to clarify the absence of O<sub>2</sub> in the photocatalytic gas phase CO<sub>2</sub> reduction on TiO<sub>2</sub>. By modifying P25-TiO<sub>2</sub> with IrO<sub>x</sub> co-catalysts it was possible to observe photocatalytic water splitting, *i.e.* the formation of gaseous O<sub>2</sub> and H<sub>2</sub> in almost stoichiometric amounts, without the use of sacrificial agents, while bare P25-TiO<sub>2</sub> showed no activity in H<sub>2</sub> and O<sub>2</sub> formation under similar reaction conditions. Investigating the effect of improved H<sub>2</sub>O oxidation properties on the photocatalytic CO<sub>2</sub> reduction revealed that the CH<sub>4</sub> formation on P25 from CO<sub>2</sub> was completely inhibited as long as the H<sub>2</sub>O splitting reaction proceeded. Furthermore, we found that a certain amount of O<sub>2</sub> is consumed under conditions of photocatalytic water oxidation. A quantification showed it to be in the same order of magnitude as the oxygen which is missing as a byproduct from photocatalytic CO<sub>2</sub> conversion. A detailed interpretation of the results in the context of the general understanding of the photocatalytic CO<sub>2</sub> reduction with H<sub>2</sub>O on TiO<sub>2</sub> allows the hypothesis that P25-TiO<sub>2</sub> undergoes a stoichiometric reaction, meaning that the CH<sub>4</sub> formation is not based on a true catalytic cycle and runs only as long as TiO<sub>2</sub> can consume oxygen.

Received 20th December 2018,  
Accepted 1st May 2019

DOI: 10.1039/c8cp07765g

rsc.li/pccp

## Introduction

The photocatalytic reduction of CO<sub>2</sub> attracted lots of attention within the last thirty years. Forming mobile energy sources by chemical reactions with CO<sub>2</sub> and the help of (sun-)light would be an important achievement for a more sustainable energy system that helps to protect the environment.<sup>1</sup> Due to the massive use of fossil fuels for energy supply and the depletion of natural reservoirs in the near future,<sup>2</sup> it is desirable to commercialize alternative ways for providing humanity with renewable energy sources.<sup>3</sup> Another important issue is the noticeable accumulation of CO<sub>2</sub> in the atmosphere as a result of the total combustion of fossil fuels.<sup>3,4</sup> An increasing CO<sub>2</sub> level accelerates the greenhouse effect and is associated with global warming and changes of the climatic conditions. Making use of CO<sub>2</sub> as a raw material could contribute to decreasing the production of anthropogenic CO<sub>2</sub> and help to use carbon-containing

energy carriers in a closed cycle. An often used term for such a reaction is “artificial photosynthesis”.<sup>5</sup>

An efficient photocatalyst needs to perform at least two functions. The first function is that of a photoabsorber, which means that the material generates charge carriers upon absorption of photons. These charge carriers must have adequate oxidation and reduction potential for the desired redox reactions.<sup>6,7</sup> It is also necessary that the charge carriers become spatially separated from each other to avoid their immediate recombination, and that they can migrate to the surface of the material. The second function is that of a heterogeneous catalyst. Therefore, it is necessary that the material exposes active sites in order to activate the reactants sufficiently to facilitate charge carrier transfer reactions. Such an activation can be initiated by adsorption of the reactants on the catalyst surface.<sup>8</sup> After decades of research TiO<sub>2</sub> is still one of the most promising and most studied materials as photocatalyst for reduction of CO<sub>2</sub>.<sup>1</sup> Indeed a number of alternative materials have been tried, but the activity of TiO<sub>2</sub>,<sup>9</sup> the non-toxicity, stability against photocorrosion<sup>10,11</sup> and the commercial availability maintain it as a meaningful candidate for photocatalytic approaches. However, performing photocatalytic CO<sub>2</sub> reduction experiments in order to gain knowledge about the mechanistic details is a challenge.<sup>12,13</sup> The examination of elementary steps, for instance, the identification of kinetic barriers or the finding

<sup>a</sup> Max Planck Institute for Chemical Energy Conversion,  
45470 Mülheim an der Ruhr, Germany. E-mail: simon.ristig@cec.mpg.de

<sup>b</sup> Leibniz Institute for Catalysis, 18059 Rostock, Germany.  
E-mail: jennifer.strunk@catalysis.de

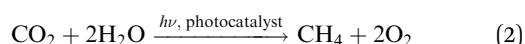
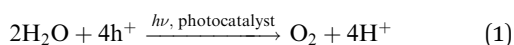
<sup>c</sup> Fritz Haber Institute of the Max Planck Society, 14195 Berlin, Germany

† Electronic supplementary information (ESI) available. See DOI: 10.1039/c8cp07765g



of details about the structure–function relationships of photocatalysts is often limited by their low activity in product formation and the detection limit of many standard analytical methods and tools.<sup>14</sup> For this reason the mechanism of this highly complex reaction is not well understood.<sup>15–18</sup>

In many reports the main products of photocatalytic CO<sub>2</sub> reduction are CH<sub>4</sub>, CO and methanol.<sup>14,19–21</sup> Given that CH<sub>4</sub> is formed from CO<sub>2</sub> in a photocatalytic reduction, it is necessary that the C=O double bonds are cleaved and four C–H bonds are formed. This process requires the transfer of eight electrons from TiO<sub>2</sub> to the carbon atom. For this reason a second reactant, which can provide these charge carriers and the source of hydrogen is needed. H<sub>2</sub>O is the most desirable oxidant for this purpose. It is commonly believed that the process of photocatalytic H<sub>2</sub>O oxidation on TiO<sub>2</sub> is associated with the transfer of four holes (h<sup>+</sup>) to form an O<sub>2</sub> molecule (1). At the same time the bound hydrogen is liberated for a subsequent hydrogenation reaction (1).



Both processes, the reduction of CO<sub>2</sub> and the oxidation of H<sub>2</sub>O produce excess oxygen as by-product which is expected to desorb from the catalyst as molecular O<sub>2</sub>. It is proposed that this excess oxygen is converted to O<sub>2</sub> (2). In the end the overall photocatalytic CO<sub>2</sub> reduction with H<sub>2</sub>O results in the formation of two equivalents of O<sub>2</sub> per CH<sub>4</sub> molecule (2). However, with some exceptions<sup>22–26</sup> the research effort focuses mostly on the formation of carbon-related products, probably as they are the targeted product for storing chemical energy. The formation of O<sub>2</sub> is often neglected, or it cannot be found at all in the products of photocatalytic CO<sub>2</sub> reduction.<sup>27,28</sup> The absence of O<sub>2</sub> can have several reasons, for instance, the participation in the backwards reaction (CH<sub>4</sub> oxidation), the replenishment of oxygen vacancies (O<sub>v</sub>) on TiO<sub>2</sub><sup>29,30</sup> and limitations in H<sub>2</sub>O oxidation kinetics leading to the accumulation of reaction intermediates on the catalyst surface. The latter could be related to the overpotential of H<sub>2</sub>O oxidation on bare TiO<sub>2</sub>.<sup>31</sup> Without using an external bias the activity towards H<sub>2</sub>O oxidation might be rather low. Then it would be questionable if there is any other hydrogen source for C–H bond formation, such as surface hydroxyl groups.

In our previous studies<sup>32,33</sup> we performed continuous flow CO<sub>2</sub> reduction experiments where we demonstrated that CH<sub>4</sub> formation is dependent on the availability of CO<sub>2</sub> and H<sub>2</sub>O. Without dosing of H<sub>2</sub>O, the product formation diminished after a couple of hours and initiated again as a pulse of H<sub>2</sub>O was given into the reactor. It was concluded that the reaction proceeds initially by the contribution of physisorbed H<sub>2</sub>O residues, which are usually available on the surface of TiO<sub>2</sub>.<sup>34,35</sup> The product formation ceases once they are consumed for hydrogenation or light-induced thermal desorption. Then the pulse-dosed H<sub>2</sub>O molecules serve as the source of hydrogenation. Although H<sub>2</sub>O appears to participate in the photoinduced CH<sub>4</sub>

formation, it was not possible to detect any O<sub>2</sub> or oxygen-derived species as products of H<sub>2</sub>O oxidation. On this account the present study focuses on the clarification of the fate of O<sub>2</sub> as the by-product of the overall photocatalytic CO<sub>2</sub> reduction.

The most prominent materials for H<sub>2</sub>O oxidation in electrochemical approaches are IrO<sub>x</sub> and CoO<sub>x</sub>. It has been found that these transition metal oxides exhibit an outstanding activity in this reaction because of their relatively low overpotential.<sup>36–39</sup> Investigations on IrO<sub>x</sub> and CoO<sub>x</sub> materials have shown that the activity in the OER is dependent on the concentration of lattice defects.<sup>36,40</sup> A study on hydrated amorphous Ir oxyhydrates<sup>40</sup> revealed that IrO<sub>x</sub> species having defects in the cationic and anionic lattice structure are more active in the OER. The authors concluded that weakly bound electrophilic oxygen species play a key role in the superior activity. In order to form such electrophilic oxygen species the surrounding Ir lattice requires flexible oxidation states.<sup>40</sup> The electrophilic oxygen species are prone to nucleophilic attacks of H<sub>2</sub>O. It is assumed that these species participate in the potential limiting step, namely the O–O bond formation of the OER.<sup>40,41</sup> Furthermore the photocatalytic activity of IrO<sub>x</sub> as a co-catalyst for the O<sub>2</sub> evolution reaction has also been tested. It is proposed that photogenerated holes in TiO<sub>2</sub> are transferred to the IrO<sub>x</sub> particles,<sup>42,43</sup> where the H<sub>2</sub>O oxidation reaction takes place. In this way TiO<sub>2</sub> represents the photoabsorber and IrO<sub>x</sub> the heterogeneous catalyst. Such IrO<sub>x</sub>/TiO<sub>2</sub> materials showed an improved O<sub>2</sub> evolution activity compared to bare TiO<sub>2</sub>.<sup>42</sup> On this account it appears to be a suitable candidate for modification of P25 TiO<sub>2</sub> with an O<sub>2</sub> evolution co-catalyst, in order to evaluate if improved H<sub>2</sub>O oxidation conditions have an effect towards the overall product formation of photocatalytic CO<sub>2</sub> reduction to CH<sub>4</sub>. At the same time the impact of O<sub>2</sub> evolution on CH<sub>4</sub> formation can be investigated. This elucidation helps to verify if product formation is a true catalytic cycle. Furthermore, it contributes to a better understanding of this complicated process and assists the development of reaction-based modification strategies for photocatalyst preparation.

## Results

### Photocatalytic cleaning and H<sub>2</sub>O splitting with IrO<sub>x</sub>/P25

The results of photocatalytic H<sub>2</sub>O splitting experiments with the 0.05 wt% IrO<sub>x</sub>/P25 samples calcined at 400 and 200 °C, respectively are shown in Fig. 1 and 2. A significant H<sub>2</sub> formation can be observed for both samples once the illumination is started at 0 h (Fig. 1 and 2). It can also be seen that the H<sub>2</sub> formation rates scale with the flow rates of H<sub>2</sub>O and stabilize over the course of the experiment. In contrast O<sub>2</sub> formation shows a different development. O<sub>2</sub> is only detected after 6 h of illumination in the first experiment of the 400 °C sample (Fig. 1A). For this reason a second H<sub>2</sub>O splitting experiment with this sample is conducted (Fig. 1B). In this experiment the apparent O<sub>2</sub> formation rate increases strongly from 0 to 3.75 h. From 3.75 h on, the formation rate of O<sub>2</sub> appears to be unsteady and the ratio between the evolution of O<sub>2</sub> and H<sub>2</sub> is approximately 1 : 3.



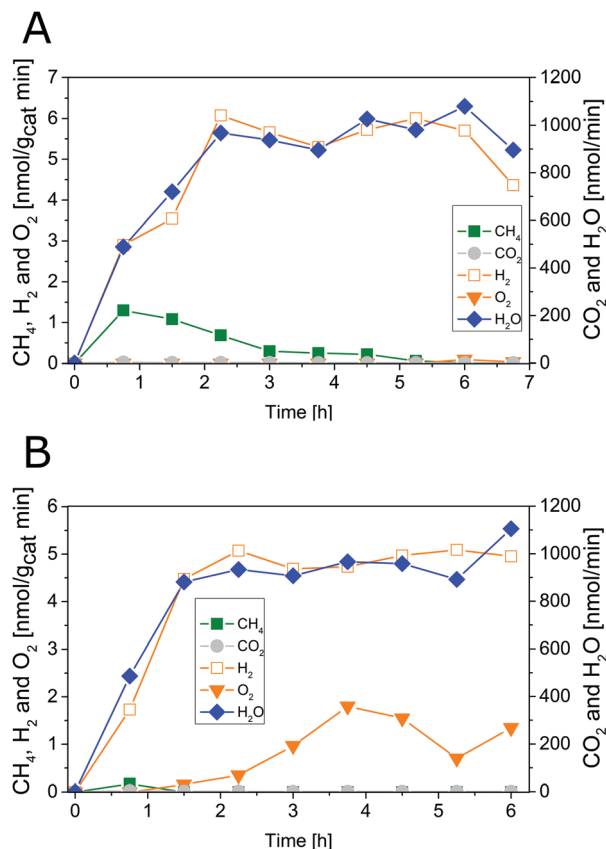


Fig. 1 Photocatalytic H<sub>2</sub>O splitting with 0.05 wt% IrO<sub>x</sub>/P25 calcined at 400 °C, irradiation time: 6.75 h; (A) first experiment, (B) second experiment. Lines are included in order to guide the eye.

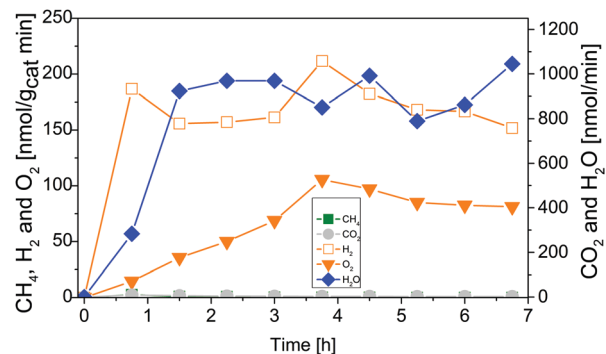


Fig. 2 Photocatalytic H<sub>2</sub>O splitting with 0.05 wt% IrO<sub>x</sub>/P25 calcined at 200 °C. Irradiation time: 6.75 h. Lines are included in order to guide the eye.

The 200 °C calcined sample shows also an increase of the apparent O<sub>2</sub> formation rate from 0 to 3.75 h (Fig. 2). Moreover, the product formation rates after 3.75 h reveal a O<sub>2</sub> : H<sub>2</sub> ratio of approximately 1 : 2.

From 5.25 to 6.75 h (Fig. 2) the product formation becomes relatively stable so that steady-state conditions are almost reached. However, it is questionable why the apparent O<sub>2</sub> formation starts delayed to the H<sub>2</sub> formation. Another important observation is the difference in the overall activity

of the two samples. It can be noticed that the 200 °C sample is about 30 times more active in H<sub>2</sub> formation than the 400 °C sample. Thus, the calcination temperature seems to have a distinct influence on the catalytic properties of the IrO<sub>x</sub>/P25 samples.

The reference P25 samples were also tested with respect to their performance in photocatalytic H<sub>2</sub>O splitting. From Fig. 3A and B it can be observed that the samples show no measureable activity in the formation of O<sub>2</sub> and H<sub>2</sub>. The results of the modified samples indicate that IrO<sub>x</sub> positively influences the formation of H<sub>2</sub> and O<sub>2</sub>.

#### Photocatalytic cleaning and H<sub>2</sub>O splitting with CoO<sub>x</sub>/P25

In contrast to the IrO<sub>x</sub>-modified P25 samples, the CoO<sub>x</sub> modified samples show a significantly different activity in the photocatalytic H<sub>2</sub>O splitting reaction. From Fig. S1A and B (ESI<sup>†</sup>) it can be observed that only the sample calcined at 200 °C showed activity in H<sub>2</sub> formation. Furthermore it can be seen that the activity in H<sub>2</sub> formation ceases over the time of illumination (Fig. S1A, ESI<sup>†</sup>). Both samples, the 200 °C and 400 °C sample, did not exhibit any activity in O<sub>2</sub> formation. The 400 °C samples displayed no activity in the H<sub>2</sub> and O<sub>2</sub> formation. Due to the absence of activity in O<sub>2</sub> formation, the samples were not further tested in the photocatalytic CO<sub>2</sub> reduction.

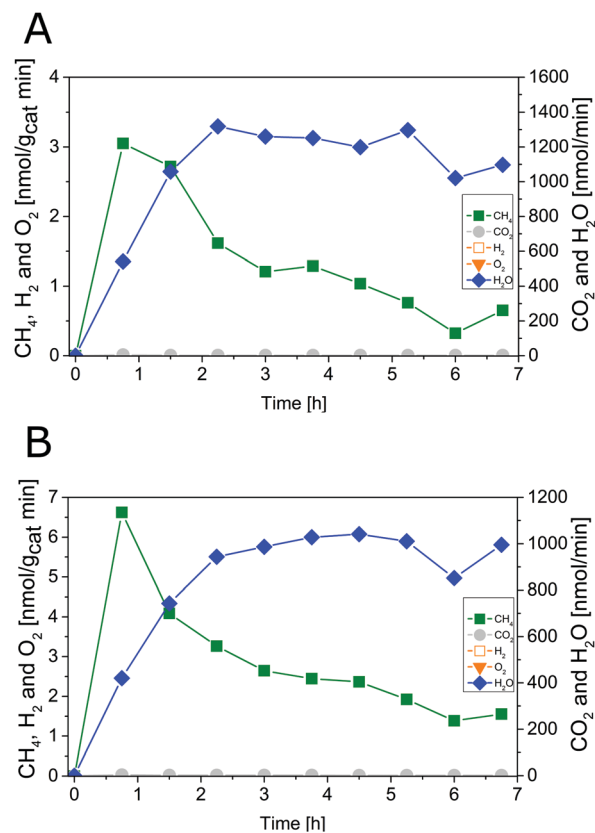


Fig. 3 Photocatalytic H<sub>2</sub>O splitting with (A) P25 reference sample calcined at 200 °C. (B) P25 reference sample calcined at 400 °C. Irradiation time: 6.75 h. Lines are included in order to guide the eye.



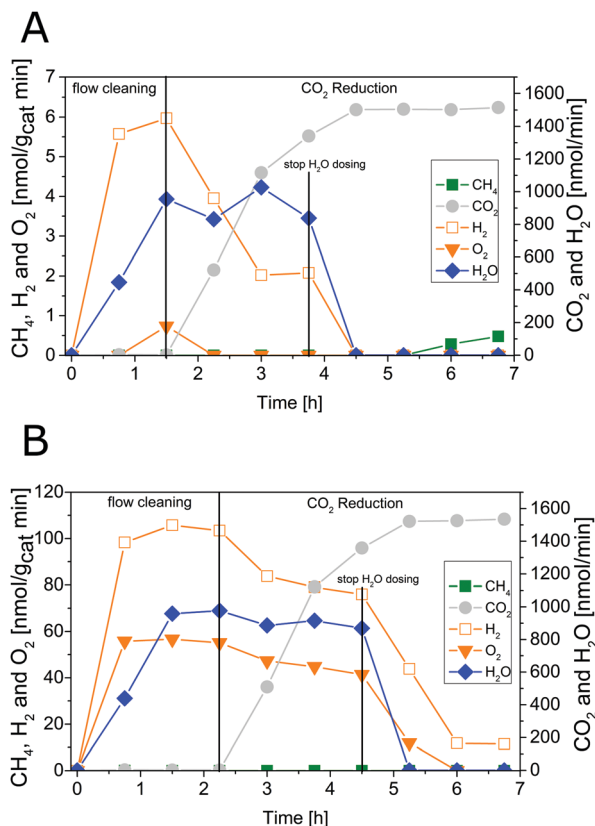


Fig. 4 Photocatalytic  $\text{CO}_2$  reduction with 0.05 wt%  $\text{IrO}_x/\text{P25}$  calcined at (A) 400 °C (flow cleaning from 0 to 1.5 h,  $\text{CO}_2$  reduction from 1.5 h to 6.75 h,  $\text{H}_2\text{O}$  dosing from 0 to 3.75 h) and (B) 200 °C (flow cleaning from 0 to 2.25 h,  $\text{CO}_2$  reduction from 2.25 h to 6.75 h,  $\text{H}_2\text{O}$  dosing from 0 to 4.5 h). Lines are included in order to guide the eye.

### Photocatalytic $\text{CO}_2$ reduction with $\text{IrO}_x/\text{P25}$

Fig. 4 shows results of combined flow cleaning and photocatalytic  $\text{CO}_2$  reduction experiments with the  $\text{IrO}_x/\text{P25}$  samples. Both samples show significant activity in the formation of  $\text{H}_2$  and  $\text{O}_2$  before the  $\text{CO}_2$  dosing was initiated. The formation rate of these products decreases once  $\text{CO}_2$  is flushed through the reactor, although the water concentration remained fairly constant. In case of the sample calcined at 400 °C the rate of  $\text{H}_2$  was more than halved within 3.25 h of  $\text{CO}_2$  dosing, while  $\text{O}_2$  was completely absent (Fig. 4A) in the products. These observations are less pronounced for the 200 °C sample (Fig. 4B) so that only a slight decrease of both rates was observed. However, under the applied reaction conditions it was not possible to detect  $\text{CH}_4$  as a product of  $\text{CO}_2$  reduction. It rather seems that  $\text{CO}_2$  has primarily a negative impact on the  $\text{H}_2$  and  $\text{O}_2$  formation in a way that generation of products is markedly disturbed. The dosing of  $\text{H}_2\text{O}$  was stopped after 3.25 h of  $\text{CO}_2$  reduction, to probe if the absence of this reactant makes a difference in the overall selectivity. From Fig. 4 it can be seen that the absence of  $\text{H}_2\text{O}$  in the gas flow strongly affects the  $\text{H}_2$  and  $\text{O}_2$  formation. A clear decrease of both formation rates can be seen. More specific, it can be noticed that no  $\text{H}_2$  and  $\text{O}_2$  evolution takes place for the 400 °C sample. In case of the 200 °C sample, the  $\text{O}_2$  formation declines completely while that of  $\text{H}_2$  drops down to a

constant rate. However, after the  $\text{H}_2\text{O}$  dosing was stopped it was possible to observe formation of  $\text{CH}_4$ , at least for the 400 °C sample. Thereby the rate increased from 5.25 to 6.75 h (Fig. 4A). In contrast the 200 °C sample showed no  $\text{CH}_4$  formation under the applied reaction conditions.

The intensive dosing of  $\text{H}_2\text{O}$  during activity studies could result in an accumulation of this reactant on the surface of  $\text{TiO}_2$  based photocatalysts, which can limit its activity in  $\text{CO}_2$  reduction.<sup>32</sup> In order to investigate this potential limitation, a similar experiment with the 200 °C sample was carried out with a reduced  $\text{H}_2\text{O}$  flow rate of  $\sim 25 \text{ nmol min}^{-1}$ . With these conditions bare P25 showed the highest  $\text{CO}_2$  reduction activity in our previous studies.<sup>32</sup> The results of the flow cleaning and  $\text{CO}_2$  reduction experiments are displayed in Fig. S2 (ESI<sup>†</sup>) and Fig. 5, respectively, and reveal a significant activity in the  $\text{H}_2$  and  $\text{O}_2$  formation with the reduced amounts of  $\text{H}_2\text{O}$ . After adding  $\text{CO}_2$  to the gas flow the apparent  $\text{O}_2$  formation ceases completely, while  $\text{H}_2$  formation decreases to a stable rate. It was again not possible to detect any  $\text{CH}_4$  formation (Fig. 5). The pure P25 references, without  $\text{IrO}_x$  or  $\text{CoO}_x$ , showed significant activity in  $\text{CH}_4$  formation when  $\text{CO}_2$  was given to the reactor (Fig. S3A and B, ESI<sup>†</sup>). The activity of the sample calcined at 200 °C (Fig. S3A, ESI<sup>†</sup>) was higher than that of the 400 °C sample (Fig. S3B, ESI<sup>†</sup>). This observation is similar to the activity of the  $\text{IrO}_x/\text{P25}$  samples in  $\text{H}_2\text{O}$  splitting (Fig. 1 and 2). The P25 reference samples however exhibited no activity in  $\text{H}_2$  and  $\text{O}_2$  formation at all (Fig. 3). These findings are in accordance with our previous studies on photocatalytic  $\text{CO}_2$  reduction with P25.<sup>32,33</sup> In a consecutive experiment with the P25 references it was investigated if a similarly delayed initiation of  $\text{O}_2$  evolution can be observed during  $\text{CH}_4$  formation, as it was observed for the  $\text{IrO}_x/\text{P25}$  samples. Therefore a combined flow cleaning and  $\text{CO}_2$  reduction experiment was carried out with the sample calcined at 400 °C (Fig. 6) for an extended period of 18 h. To prevent an inhibition of  $\text{CH}_4$  formation by extensive accumulation or a complete lack of  $\text{H}_2\text{O}$ , repetitive pulse dosing of  $\text{H}_2\text{O}$  was performed in order to provide suitable conditions to run  $\text{CH}_4$  formation over an appropriate period of time. It can be obviously seen in Fig. 6 that after about 6 h the pulses of  $\text{H}_2\text{O}$  initially decrease the rate of  $\text{CH}_4$  formation.

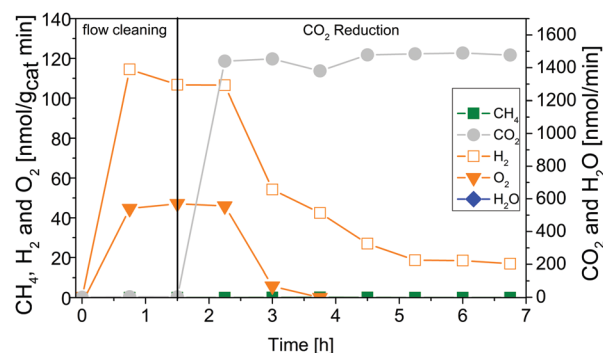


Fig. 5 Photocatalytic  $\text{CO}_2$  reduction with 0.05 wt%  $\text{IrO}_x/\text{P25}$  calcined at 200 °C (flow cleaning from 0 to 1.5 h,  $\text{CO}_2$  reduction from 1.5 h to 6.75 h,  $\sim 25 \text{ nmol min}^{-1}$   $\text{H}_2\text{O}$  dosing from 0 to 6.75 h). Lines are included in order to guide the eye.



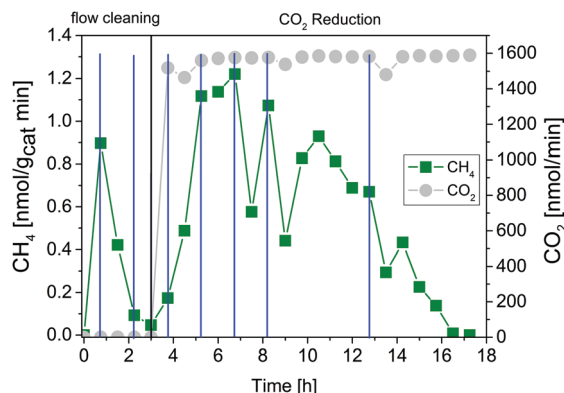


Fig. 6 Photocatalytic CO<sub>2</sub> reduction with P25 calcined at 400 °C (flow cleaning from 0 to 3 h, CO<sub>2</sub> reduction from 3 h to 17.75 h, pulse dosing of H<sub>2</sub>O indicated by blue dashes). Lines are included in order to guide the eye.

However, a significant increase of the CH<sub>4</sub> formation can be observed in each of the subsequent GC analysis cycles. In total it was possible to observe CH<sub>4</sub> formation over a period of 14.25 h (Fig. 6). Under the applied reaction conditions the CH<sub>4</sub> formation rate decreases over the course of the CO<sub>2</sub> reduction experiment. There was no activity left after 17.75 h (Fig. 6). As no delayed O<sub>2</sub> formation could be detected during the experiment it seems that, in contrast to the H<sub>2</sub>O splitting experiments on IrO<sub>x</sub>/P25, bare P25 does not release any molecular oxygen in a similar range of time.

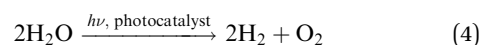
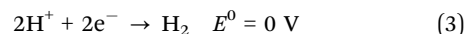
## Discussion

The results can be discussed in the context of the general understanding of photocatalytic energy conversion reactions on TiO<sub>2</sub>-based materials. Then, a detailed insight into the mode of action can be obtained for IrO<sub>x</sub>/TiO<sub>2</sub> and some hypotheses on the reaction progress on TiO<sub>2</sub> can be formulated.

### Photocatalytic cleaning and H<sub>2</sub>O splitting on IrO<sub>x</sub>/P25

The IrO<sub>x</sub>-modified P25 samples showed a noticeable activity in the formation of H<sub>2</sub> and O<sub>2</sub>. Due to the strong dependence of the activity from the dosing of H<sub>2</sub>O and the O<sub>2</sub>:H<sub>2</sub> ratio of approximately 1:2, it is assumed that the product formation originates from overall photocatalytic H<sub>2</sub>O splitting (4). This is a meaningful result showing that the stoichiometric H<sub>2</sub>O splitting in a gas-solid process has been realized, since no external bias or any sacrificial agents were used in order to improve the formation rates of H<sub>2</sub> and O<sub>2</sub>. Furthermore, it is possible to observe the simultaneous formation of both products in one high-purity reaction chamber. However, it is questionable how the product formation is realized on IrO<sub>x</sub>/P25 and which charge carrier dynamic processes are involved. A hypothetical approach to explain the activity of IrO<sub>x</sub>/P25 can be based on the two main functions of a photocatalyst. In this sense TiO<sub>2</sub> represents the photoabsorber, where mobile charge carriers are generated under absorption of UV photons. Some of the photogenerated h<sup>+</sup> escape from recombination and migrate to the IrO<sub>x</sub> particles, where they catalyze the oxidation of H<sub>2</sub>O to O<sub>2</sub> (1). In this way IrO<sub>x</sub> represents the function of the

heterogeneous catalyst. This has been well documented in liquid-phase H<sub>2</sub>O splitting. The separation of charge carriers over the interface of TiO<sub>2</sub> and IrO<sub>x</sub> enhances their lifetime, thus it is beneficial for the light efficiency of the overall H<sub>2</sub>O splitting reaction (4). The H<sup>+</sup> formed from H<sub>2</sub>O oxidation (1) are then reduced to H<sub>2</sub> gas (3). Since the electrons are left behind in TiO<sub>2</sub>, this reaction is likely to proceed on the TiO<sub>2</sub> surface. For this purpose TiO<sub>2</sub> must expose sites which can transfer electrons. It appears that such sites are available and their accessibility is maintained even under continuous flow conditions and accumulation of H<sub>2</sub>O on the surface of TiO<sub>2</sub>, since the activity of H<sub>2</sub> formation is almost stable during the H<sub>2</sub>O splitting experiments.



With respect to H<sub>2</sub> formation, the catalytic functionality is inherent to TiO<sub>2</sub>, as has been observed earlier, and a modification with a co-catalyst does not seem to be needed to generally allow this reaction.<sup>44</sup> The functionalization of TiO<sub>2</sub> with co-catalysts, especially Pt, is however a common approach to improve the H<sub>2</sub> formation capability for significantly higher H<sub>2</sub> yields.<sup>45</sup>

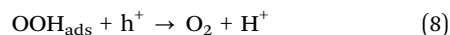
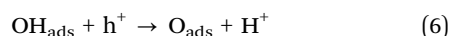
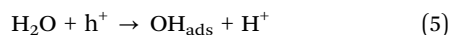
According to the hypothetical approach in the previous chapter to explain the activity of IrO<sub>x</sub>/P25 it is expected that the H<sub>2</sub>O oxidation reaction similarly proceeds on CoO<sub>x</sub> and the formation of H<sub>2</sub> on TiO<sub>2</sub>. In Fig. S1A and B (ESI<sup>†</sup>) it was shown that only the sample calcined at 200 °C showed activity in H<sub>2</sub> formation. However, the fact that H<sub>2</sub> was formed indicates that a hydrogen source has been provided by photocatalytic H<sub>2</sub>O oxidation. The interface between TiO<sub>2</sub> and CoO<sub>x</sub> can potentially cause an insufficient hole transfer between the photoabsorber and the co-catalyst which lowers the activity of H<sub>2</sub>O oxidation. Furthermore the reaction pathway of photocatalytic H<sub>2</sub>O oxidation on CoO<sub>x</sub> will be different compared to IrO<sub>x</sub>. Therefore it is possible that specific steps in the overall reaction mechanism cannot be activated sufficiently to allow an efficient O<sub>2</sub> formation. As a consequence H<sub>2</sub>O is only oxidized partly, so that the resulting oxygen-derived intermediates remain on CoO<sub>x</sub>, without being further oxidized to O<sub>2</sub> gas. In this way the oxygen-derived intermediates might prevent further oxidation of H<sub>2</sub>O, which lowers the activity over time as it was observed in Fig. S1A (ESI<sup>†</sup>).

### Potential reasons for the lack of CH<sub>4</sub> formation on IrO<sub>x</sub>/TiO<sub>2</sub>

The CO<sub>2</sub> reduction experiments with the IrO<sub>x</sub>/P25 samples displayed no measurable activity in CH<sub>4</sub> formation. Instead, O<sub>2</sub> and H<sub>2</sub> formation are the dominant processes and only small amounts of CH<sub>4</sub> can be formed if H<sub>2</sub>O dosing is stopped (Fig. 4A). This observation is in stark contrast to the reference samples. It is highly probable that the improved H<sub>2</sub>O splitting conditions by the IrO<sub>x</sub> modification are responsible for the absence of CH<sub>4</sub> formation. In the following it will be elucidated in which ways the H<sub>2</sub>O oxidation reaction might affect the CO<sub>2</sub> reduction reaction.

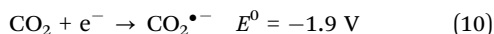
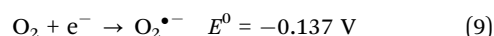


The oxidation of H<sub>2</sub>O to O<sub>2</sub> is often represented by four single step reactions (5)–(8).<sup>31,46–48</sup>



Each of these steps comprises the transfer of one h<sup>+</sup>. Species such as hydroxyl- (5), oxygen adatom- (6) and hydroperoxyl-species (7) are formed as intermediates. Especially the hydroxyl and peroxy species are highly reactive oxygen species and have potential to promote the backward reaction of CO<sub>2</sub> reduction, which is hydrocarbon oxidation.

Aside from hydrocarbon oxidation, another explanation for the absence of CH<sub>4</sub> formation could be based on a competition for charge carriers. For instance the reduction of O<sub>2</sub> (9) and the generation of H<sub>2</sub> (3) are also electron consuming reactions. It is questionable which of these processes is associated with the lowest barrier and is thus more likely to proceed. Due to a lack of knowledge on activation barriers, the redox potentials of the particular reactions are regarded as a first approximation.



For a reaction with CO<sub>2</sub> the commonly proposed one electron transfer<sup>7</sup> is considered to be the rate limiting step. The comparison of the redox potentials reveals that CO<sub>2</sub> reduction (10) is the thermodynamically least favored process.<sup>49–51</sup> It needs to be stressed that reaction (10) is virtually not possible thermodynamically on any semiconducting material, because conduction band minima are not located at sufficiently negative potential.<sup>7</sup> This one electron transfer can only proceed if, for instance, the adsorption of the CO<sub>2</sub> molecule leads to a slightly bent structure, activating the CO<sub>2</sub> and facilitating further reactions. As a consequence of the extreme stability of CO<sub>2</sub> it is highly probable that the photogenerated charge carriers are more likely consumed by H<sub>2</sub> evolution and O<sub>2</sub> reduction, so that fewer electrons are available for reduction of CO<sub>2</sub>. Hence the activity of TiO<sub>2</sub> in CH<sub>4</sub> formation could be negatively influenced. Such a competition for charge carriers would also explain the decrease in water splitting activity of IrO<sub>x</sub>/TiO<sub>2</sub> when CO<sub>2</sub> is added to the reaction mixture (Fig. 4A and 5). In a related manner, bicarbonates, which may be formed in presence of CO<sub>2</sub> on the TiO<sub>2</sub> surface, have been proposed as hole trap sites.<sup>52</sup> This represents an alternative mechanism by which competition for charge carriers, holes in this case, might occur.

The absence of CH<sub>4</sub> formation in the presence of a highly active co-catalyst for O<sub>2</sub> evolution due to reactive oxygen species and competitive charge transfer reaction appears to be plausible.

As a third possible explanation it should be considered that at least one potential mechanism suggested for CO<sub>2</sub> reduction to CH<sub>4</sub> on TiO<sub>2</sub>, namely the glyoxal pathway,<sup>18</sup> contains not only reductive but also oxidative elementary steps. If such a

mechanism is in operation, it will no longer be possible on TiO<sub>2</sub> if all holes are transferred to IrO<sub>x</sub>.

### H<sub>2</sub>O oxidation on IrO<sub>x</sub>/TiO<sub>2</sub> and fate of oxygen

What makes the results of the IrO<sub>x</sub>/P25 sample significantly more interesting is the activity in the H<sub>2</sub> formation as a consequence of the improved H<sub>2</sub>O oxidation properties, together with the delayed O<sub>2</sub> formation rate in the initial phase of the flow cleaning experiments. The obtained results provide specific information about the photocatalytic properties of TiO<sub>2</sub>. Those will later be used to explain product formation of photocatalytic CO<sub>2</sub> reduction on TiO<sub>2</sub>.

The results with IrO<sub>x</sub>/P25 (Fig. 1, 2 and 4) indicated that not all O<sub>2</sub> produced from H<sub>2</sub>O oxidation was detected over the course of the experiment. In case of CO<sub>2</sub> reduction on P25 it was even not possible to detect any O<sub>2</sub>. For this reason the deficient amount of O<sub>2</sub> was determined for the IrO<sub>x</sub>/P25 and P25 samples calcined at 400 °C. At first the absent amount of O<sub>2</sub> is calculated for IrO<sub>x</sub>/P25. For this purpose the overall H<sub>2</sub> formation and the O<sub>2</sub>:H<sub>2</sub> ratio of 1:2 as proposed in reaction (4) are used. The difference between the theoretically expected (O<sub>2</sub> theoretical) and the detected amount (O<sub>2</sub> detected) corresponds to the amount of O<sub>2</sub> which was not found (O<sub>2</sub> absent) in the gas-phase of the photoreactor (Table 1).

In order to realize a reliable comparison to the absent amount of O<sub>2</sub> in CO<sub>2</sub> reduction, it would be necessary to run the reaction until stoichiometric formation of both products can be observed, too. However, the CH<sub>4</sub> formation ceased after 14.25 h of CO<sub>2</sub> reduction (Fig. 6). Consequently it is solely possible to determine the theoretically expected amount of O<sub>2</sub> to this point of time. The calculation was performed under consideration of the stoichiometry in reaction (2). Thereby the molar amount of O<sub>2</sub> corresponds to twice the molar amount of CH<sub>4</sub> (Table 2).

The comparison of the balances (Tables 1 and 2) reveals that the absent amounts of O<sub>2</sub> in both the H<sub>2</sub>O splitting reaction with IrO<sub>x</sub>/P25 (Fig. 1) and the CO<sub>2</sub> reduction with bare P25 (Fig. 6) are at least in the same order of magnitude. On this account it appears realistic that the observed phenomena are based on the same effect. The present study uses a GC as the analytical device so that only the gas phase of the photoreactor can be analyzed. Hence, the absence of O<sub>2</sub> in the analysis is either indicative for the absence of its formation or the consumption by the sample.

**Table 1** Calculation of absent O<sub>2</sub> in the flow cleaning experiments with the 0.05 wt% IrO<sub>x</sub>/P25 (400 °C); 70 mg of sample was used

	Molar amount [nmol]
H <sub>2</sub>	247
O <sub>2</sub> theoretical	123.5
O <sub>2</sub> detected	20
O <sub>2</sub> absent	103.5

**Table 2** Calculation of absent O<sub>2</sub> in the flow cleaning experiments with P25 (400 °C); 70 mg of sample was used

	Molar amount [nmol]
CH <sub>4</sub>	39
O <sub>2</sub> absent	78



The obtained results are the basis to hypothesize the fate of oxygen in photocatalytic reaction on  $\text{TiO}_2$ .

### Plausible conclusions on the mode of action of $\text{TiO}_2$ in photocatalytic $\text{CO}_2$ reduction

In contrast to the  $\text{IrO}_x$ -modified samples, the reference P25 samples exhibited a significant activity in the  $\text{CH}_4$  formation. At the same time there was no observable activity in the  $\text{H}_2\text{O}$  splitting reaction. In general, the photocatalytic  $\text{H}_2\text{O}$  oxidation is thermodynamically possible on bare  $\text{TiO}_2$ . Kinetic barriers in the overall reaction cycle might result in a very small apparent rate when no co-catalyst is used. Although no indication for water splitting is observed for bare  $\text{TiO}_2$  our previous work has shown that the presence of water is required for  $\text{CH}_4$  formation from photocatalytic  $\text{CO}_2$  reduction. Therefore, water is still expected to deliver hydrogen for  $\text{CH}_4$  formation. Considering that the proposed elementary steps of  $\text{H}_2\text{O}$  oxidation (5)–(8) all liberate  $\text{H}^+$ , a hydrogen source is generated even if the final  $\text{O}_2$  evolution step is kinetically hindered. From the results with the  $\text{IrO}_x/\text{P25}$  samples it can be concluded that such a source of hydrogen should be rapidly reduced to  $\text{H}_2$  on  $\text{TiO}_2$ . However, on bare  $\text{TiO}_2$  we did not observe  $\text{H}_2$  formation, so it is questionable if any of the generally assumed steps of  $\text{H}_2\text{O}$  oxidation occurs under the applied reaction conditions. If this is not the case, a different source of protons than photocatalytic  $\text{H}_2\text{O}$  oxidation needs to participate in C–H bond formation. Moreover, the results of the present study revealed that  $\text{CH}_4$  formation only proceeds when no  $\text{H}_2\text{O}$  is oxidized and the by-product  $\text{O}_2$  is absent in the gas-phase. This correlation is in conflict with the proposed reaction eqn (2).

Based on our results, product formation in photocatalytic  $\text{CO}_2$  reduction coupled to oxygen consumption by  $\text{TiO}_2$  is suggested as likely explanation. One feasible way for such consumption is the replenishment of oxygen vacancies ( $\text{O}_v$ ). From experimental studies<sup>53–55</sup> it is known that  $\text{O}_2$  dissociates and can undergo reactions with  $\text{O}_v$  on the surface of  $\text{TiO}_2$  under room temperature conditions. Since all experiments of this study were performed under such conditions and the amount of absent  $\text{O}_2$  is very small, it is proposed that the replenishment of  $\text{O}_v$  may explain the fate of this by-product. The obtained results of the  $\text{IrO}_x/\text{P25}$  samples showed that  $\text{O}_2$  formation started delayed to the  $\text{H}_2$  formation. The replenishment of  $\text{O}_v$  may be the reason why fractions of  $\text{O}_2$  were temporarily not detectable in the gas phase. Once all defects are healed the release of the entire amount of  $\text{O}_2$  from the surface of the photocatalyst initiates, so the formation rates converged to the stoichiometric ratio of  $\text{H}_2\text{O}$  splitting. Another explanation for the initially missing gas-phase oxygen not further discussed here could be a formation of peroxide species adsorbed on the catalyst surface. The adsorption<sup>56,57</sup> and reactions<sup>57</sup> of peroxide species, possibly also formed in a gas-phase  $\text{H}_2\text{O}$  splitting reaction on  $\text{TiO}_2$ , has been examined in detail by comprehensive theoretical studies. Hydrogen peroxide has also been identified as origin for an oxygen deficit in liquid-phase photocatalytic water splitting over  $\text{Pt}/\text{TiO}_2$ .<sup>58</sup>

The overall  $\text{CO}_2$  reduction is proposed to include two processes forming  $\text{O}_2$ . On the one hand side the formation of

$\text{CH}_4$  by reduction of  $\text{CO}_2$ , on the other hand side the oxidation of  $\text{H}_2\text{O}$  to generate the source of hydrogen for C–H bond formation. Assuming that oxygen vacancies are responsible for the absence of  $\text{O}_2$ , these point defects are strongly associated with the photocatalytic activity of  $\text{TiO}_2$ . In one of our studies<sup>33</sup> it was verified that the presence of  $\text{O}_2$  in the gas-phase of the reaction gas atmosphere induces an inhibition of  $\text{CH}_4$  formation. Since oxygen-derived species from  $\text{CO}_2$  reduction are also suspected to affect the  $\text{CH}_4$  formation negatively, a replenishment of  $\text{O}_v$  might avoid that gaseous  $\text{O}_2$  and potentially reactive oxygen-derived intermediates inhibit the  $\text{CH}_4$  formation.

Even though  $\text{H}_2\text{O}$  oxidation according to the generally accepted mechanism is not likely to occur on bare P25- $\text{TiO}_2$ , the  $\text{CH}_4$  formation has been proven to require the presence of  $\text{H}_2\text{O}$ .<sup>32</sup> For this reason an alternative pathway for liberation of the hydrogen in  $\text{H}_2\text{O}$  must be considered. In general, surface hydroxyl groups are naturally present on the surface of  $\text{TiO}_2$  and can be formed by dissociative adsorption of  $\text{H}_2\text{O}$  in a  $\text{O}_v$  (11).



The surface OH-groups represent hydrogen-containing species which are available in high concentration. If they would be sufficiently Brønsted acidic to hydrogenate, for instance carbonaceous radicals as intermediates from  $\text{CO}_2$  reduction, they could participate in product formation. Additionally, the dissociative  $\text{H}_2\text{O}$  adsorption illustrates a pathway which is consistent with the dependency of  $\text{CH}_4$  formation from  $\text{H}_2\text{O}$  and the absence of  $\text{O}_2$  formation.

Anyway, the irreversible replenishment of vacant positions by excess oxygen from  $\text{CO}_2$  or  $\text{H}_2\text{O}$  is an example for a stoichiometric reaction of the photocatalyst. Most likely the photocatalytic activity in  $\text{CO}_2$  reduction will be diminished as soon as all vacancies are healed. The observed termination of the  $\text{CH}_4$  formation in the  $\text{CO}_2$  reduction after 14.25 h (Fig. 6) underlines this hypothesis. Overall, the results indicate that the  $\text{CH}_4$  formation is presumably not based on a complete catalytic cycle including both the photocatalytic  $\text{CO}_2$  reduction and  $\text{H}_2\text{O}$  oxidation.

## Experimental

### High-purity gas-phase photoreactor set-up

The photocatalytic  $\text{CO}_2$  reduction experiments were carried out with a reactor set-up which works under conditions of highest purity. A detailed description of the set-up was given by Mei *et al.*<sup>12</sup> In brief, the reactor is made from stainless steel components which are usually used for ultra-high vacuum application. All tube connections are realized by VCR and CF connections, so that sealing of the overall system works grease-free. Purging of the reactor is performed by 99.9999% He gas (He 6.0). A diluted  $\text{CO}_2$  in He mixture (7000 ppm  $\text{CO}_2$  in He 6.0) is used as the reactant gas. Dosage of  $\text{H}_2\text{O}$  into the gas-phase is realized by a stainless steel saturator, which is temperature controlled. The  $\text{H}_2\text{O}$  concentration in the gas flow is adjusted





by the temperature of the saturator. Mass flow controllers are used for purging and dosing of the reactants. The powdered sample is finely distributed in a quartz vessel, which is placed in the center of the reactor. Illumination is conducted by a 200 W Hg/Xe lamp from Oriel instruments. A water-based filter is utilized to remove the IR radiation from the lamp spectrum. Product analysis is executed by a Shimadzu Tracera GC 2010 Plus. This GC is equipped with a barrier discharge ionization detector (BID), which allows quantifying CO<sub>2</sub>, CO, CH<sub>4</sub>, C<sub>2</sub>H<sub>6</sub>, H<sub>2</sub>O, O<sub>2</sub> and H<sub>2</sub> in the 0.1 ppm range. On the basis of this high sensitivity, the BID is a suitable analytical device for an application in continuous-flow photocatalytic CO<sub>2</sub> reduction.

### Sample preparation

Sample modification of P25 with IrO<sub>x</sub> and CoO<sub>x</sub> was performed *via* photodeposition in a semi-batch reactor made from quartz glass. On-top illumination was realized by a 1000 W Hg/Xe lamp. 400 mg P25 was dispersed in 200 mL H<sub>2</sub>O and ultrasonicated for one minute. Then the dispersion was given into the reactor and 20 mL of methanol were added. The precursors iridium acetate or cobalt acetate were added to the dispersion amounting to a nominal loading of 0.05 wt% Ir and Co, respectively. The reactor was sealed and deaerated with pure He gas for 1.5 h. After purging the reactor, the He flow rate was set to 20 mL min<sup>-1</sup> and the illumination was initiated. The overall deposition time was 3 h. Subsequently the dispersion was filtered and dried overnight. The obtained powder was then divided into two equal fractions. One fraction was calcined in synthetic air for 3 h at 200 °C, and the other at 400 °C, respectively, with a heating rate of 5 K min<sup>-1</sup>. Reference samples without Ir and Co have been prepared by the same procedure. Calcination of the samples is the first step to remove adsorbed carbon-containing species from the surface to prevent their potential contribution to the product formation leading to an overestimated activity.

### Sample pretreatment and CO<sub>2</sub> reduction

70 mg of each sample has been tested in a CO<sub>2</sub> reduction experiment. As the initial calcination steps are not sufficient to remove all of the carbon-containing species from the sample, further purification has been carried out before the activity test. This pretreatment step was performed in the photoreactor set-up. A He gas flow only including H<sub>2</sub>O was given through the reactor under illumination. The flow rate of H<sub>2</sub>O is adjusted to ~1000 nmol min<sup>-1</sup>. This pretreatment under photocatalytic reaction conditions is further termed as flow cleaning. Although such an experiment is mainly performed to purify the sample from carbonaceous impurities, it simultaneously provides conditions for photocatalytic H<sub>2</sub>O splitting. Thus the activity in the H<sub>2</sub>O splitting reaction is determined before CO<sub>2</sub> reduction is studied. GC measurements are conducted all 45 minutes to monitor the cleaning progress and the formation of H<sub>2</sub> and O<sub>2</sub>. After the concentration of products from the flow cleaning procedure (CH<sub>4</sub> and CO<sub>2</sub>) are sufficiently low the CO<sub>2</sub> reduction experiment is initiated. Therefore, the gas flow is changed from pure He to 1700 nmol min<sup>-1</sup> CO<sub>2</sub> in He. The H<sub>2</sub>O flow rate in the

CO<sub>2</sub> reduction experiments is either held at ~1000 nmol min<sup>-1</sup> or changed to ~25 nmol min<sup>-1</sup>. From our previous study<sup>32</sup> we know that high H<sub>2</sub>O flow rates can inhibit product formation. A flow of ~25 nmol min<sup>-1</sup> H<sub>2</sub>O is sufficient to observe significant product formation.

## Conclusions

In this study the effect of improved H<sub>2</sub>O oxidation properties on the gas-phase photocatalytic CO<sub>2</sub> reduction was studied by modifying P25 with co-catalysts for H<sub>2</sub>O oxidation. Simultaneously, potential reasons for the absence of gaseous O<sub>2</sub> as the by-product of photocatalytic CO<sub>2</sub> reduction on pure TiO<sub>2</sub> were investigated. The IrO<sub>x</sub>/P25 samples exhibited a significant activity in the overall photocatalytic H<sub>2</sub>O splitting, which was realized here in a pure gas-solid process under high-purity reaction conditions. It was possible to detect both products H<sub>2</sub> and O<sub>2</sub> in nearly stoichiometric amounts without the use of sacrificial agents. Photocatalytic CO<sub>2</sub> reduction experiments with IrO<sub>x</sub>/P25 samples revealed that CH<sub>4</sub> formation is only possible when no activity in H<sub>2</sub> and O<sub>2</sub> formation is observed. Competition for charge carriers by H<sub>2</sub> formation and the backward reaction of CO<sub>2</sub> reduction due to the presence of highly reactive oxygen species formed on IrO<sub>x</sub> appear to be responsible for the absence of CH<sub>4</sub> formation. If photogenerated electrons are favorably consumed by H<sub>2</sub> formation, but this product is not formed on bare TiO<sub>2</sub>, this might indicate that H<sub>2</sub>O oxidation is not the source of hydrogen for C-H bond formation in CO<sub>2</sub> reduction. Furthermore, the results of the H<sub>2</sub>O splitting experiments on IrO<sub>x</sub>/P25 revealed that O<sub>2</sub> and O-derived species are initially likely consumed by TiO<sub>2</sub> under photocatalytic reaction conditions. A quantification of the missing amounts of O<sub>2</sub> in the gas phase showed that a consumption of O<sub>2</sub> by TiO<sub>2</sub> could be responsible for the absence of this by-product in the CO<sub>2</sub> reduction reaction. Under this circumstance TiO<sub>2</sub> undergoes a stoichiometric reaction and the CH<sub>4</sub> formation is not a true catalytic cycle. Instead, it runs only as long as TiO<sub>2</sub> can consume oxygen. In addition the inhibiting effect of O<sub>2</sub> on the product formation of CO<sub>2</sub> reduction reveals that the consumption of this by-product is essential for the activity of TiO<sub>2</sub> in this reaction. Only then the inhibiting effect of O<sub>2</sub> and O-derived species in the photocatalytic CO<sub>2</sub> reduction is prevented.

## Conflicts of interest

There are no conflicts to declare.

## Acknowledgements

Open Access funding provided by the Max Planck Society.

## Notes and references

- 1 E. V. Kondratenko, *et al.*, *Energy Environ. Sci.*, 2013, **6**, 3112.
- 2 N. Armaroli and V. Balzani, *Energy for a sustainable world: From the oil age to a sun-powered future*, Wiley-VCH, Weinheim, 2011.



- 3 S. C. Roy, *et al.*, *ACS Nano*, 2010, **4**, 1259–1278.
- 4 R. Lal, *Energy Environ. Sci.*, 2008, **1**, 86–100.
- 5 S. Sato, T. Arai and T. Morikawa, *Inorg. Chem.*, 2015, **54**, 5105–5113.
- 6 B. Ohtani, *J. Photochem. Photobiol., C*, 2010, **11**, 157–178.
- 7 S. N. Habisreutinger, L. Schmidt-Mende and J. K. Stolarczyk, *Angew. Chem., Int. Ed.*, 2013, **52**, 7372–7408.
- 8 J. Li and N. Wu, *Catal. Sci. Technol.*, 2015, **5**, 1360–1384.
- 9 A. Di Paola, *et al.*, *J. Phys. Chem. C*, 2009, **113**, 15166–15174.
- 10 M. Anpo and J. M. Thomas, *Chem. Commun.*, 2006, 3273–3278.
- 11 J. Nowotny, *Oxide Semiconductors for Solar Energy Conversion: Titanium Dioxide*, CRC Press, 2016.
- 12 B. Mei, A. Pougin and J. Strunk, *J. Catal.*, 2013, **306**, 184–189.
- 13 M. Anpo, *et al.*, *J. Electroanal. Chem.*, 1995, **396**, 21–26.
- 14 A. Pougin, M. Dilla and J. Strunk, *Phys. Chem. Chem. Phys.*, 2016, 10809.
- 15 D. Lee and Y. Kanai, *J. Am. Chem. Soc.*, 2012, **134**, 20266–20269.
- 16 I. A. Shkrob, *et al.*, *J. Phys. Chem. C*, 2012, **116**, 9461–9471.
- 17 C. Amatore and J. M. Saveant, *J. Am. Chem. Soc.*, 1981, **103**, 5021–5023.
- 18 I. A. Shkrob, *et al.*, *J. Phys. Chem. C*, 2012, **116**, 9450–9460.
- 19 M. Anpo, *et al.*, *J. Phys. Chem. B*, 1997, **101**, 2632–2636.
- 20 N. G. Moustakas and J. Strunk, *Chem. – Eur. J.*, 2018, **24**, 12739–12746.
- 21 J. Schneider, *et al.*, *Chem. Rev.*, 2014, **114**, 9919–9986.
- 22 E. Korovin, D. Selishchev and D. Kozlov, *Top. Catal.*, 2016, **59**, 1292–1296.
- 23 K. Teramura, *et al.*, *Angew. Chem., Int. Ed.*, 2012, **51**, 8008–8011.
- 24 K. Iizuka, *et al.*, *J. Am. Chem. Soc.*, 2011, **133**, 20863–20868.
- 25 J.-C. Wang, *et al.*, *ACS Appl. Mater. Interfaces*, 2015, **7**, 8631–8639.
- 26 L. Liu, *et al.*, *ACS Catal.*, 2012, **2**, 1817–1828.
- 27 F. Saladin and I. Alxneit, *J. Chem. Soc., Faraday Trans.*, 1997, **93**, 4159–4163.
- 28 J. Tang, J. R. Durrant and D. R. Klug, *J. Am. Chem. Soc.*, 2008, **130**, 13885–13891.
- 29 H. Belhadj, *et al.*, *Phys. Chem. Chem. Phys.*, 2015, **17**, 22940–22946.
- 30 Z. Dohnalek, *et al.*, *J. Phys. Chem. B*, 2006, **110**, 6229–6235.
- 31 J. Rossmeisl, *et al.*, *J. Electroanal. Chem.*, 2007, **607**, 83–89.
- 32 M. Dilla, *et al.*, *ChemCatChem*, 2017, **9**, 4345–4352.
- 33 M. Dilla, R. Schlögl and J. Strunk, *ChemCatChem*, 2017, **9**, 696–704.
- 34 D. A. Panayotov and J. T. Yates, *Chem. Phys. Lett.*, 2005, **410**, 11–17.
- 35 R. L. Kurtz, *et al.*, *Surf. Sci.*, 1989, **218**, 178–200.
- 36 Z. Cai, *et al.*, *Adv. Energy Mater.*, 2018, **8**, 1701694.
- 37 H. Tucsuez, *et al.*, *Nano Res.*, 2013, **6**, 47–54.
- 38 C. C. L. McCrory, *et al.*, *J. Am. Chem. Soc.*, 2013, **135**, 16977–16987.
- 39 F. A. Frame, *et al.*, *J. Am. Chem. Soc.*, 2011, **133**, 7264–7267.
- 40 V. Pfeifer, *et al.*, *Chem. Sci.*, 2016, **7**, 6791–6795.
- 41 V. Pfeifer, *et al.*, *Chem. Sci.*, 2017, **8**, 2143–2149.
- 42 W.-H. Ryu, *et al.*, *J. Mater. Chem. A*, 2014, **2**, 5610–5615.
- 43 B. H. Meekins and P. V. Kamat, *J. Phys. Chem. Lett.*, 2011, **2**, 2304–2310.
- 44 Y. K. Kho, *et al.*, *J. Phys. Chem. C*, 2010, **114**, 2821–2829.
- 45 D. Y. C. Leung, *et al.*, *ChemSusChem*, 2010, **3**, 681–694.
- 46 Y.-F. Li, *et al.*, *J. Am. Chem. Soc.*, 2010, **132**, 13008–13015.
- 47 Y.-F. Li and A. Selloni, *ACS Catal.*, 2016, **6**, 4769–4774.
- 48 A. Valdes, *et al.*, *J. Phys. Chem. C*, 2008, **112**, 9872–9879.
- 49 R. van de Krol and M. Grätzel, *Photoelectrochemical Hydrogen Production*, Springer US, 2011.
- 50 J. Petlicki and T. G. M. van de Ven, *J. Chem. Soc., Faraday Trans.*, 1998, **94**, 2763–2767.
- 51 W. H. Koppenohl and J. D. Rush, *J. Phys. Chem.*, 1987, **91**, 4429–4430.
- 52 N. M. Dimitrijevic, *et al.*, *J. Am. Chem. Soc.*, 2011, **133**, 3964–3971.
- 53 M. A. Henderson, *et al.*, *J. Phys. Chem. B*, 2003, **107**, 534–545.
- 54 Y. Du, Z. Dohnalek and I. Lyubinetsky, *J. Phys. Chem. C*, 2008, **112**, 2649–2653.
- 55 S. Tan, *et al.*, *J. Am. Chem. Soc.*, 2011, **133**, 2002–2009.
- 56 H. Alghamdi, *et al.*, *Surf. Sci.*, 2018, **669**, 103–113.
- 57 W.-F. Huang, *et al.*, *J. Comput. Chem.*, 2011, **32**, 1065–1081.
- 58 V. Daskalaki, *et al.*, *Chem. Eng. J.*, 2011, **170**, 433–439.

